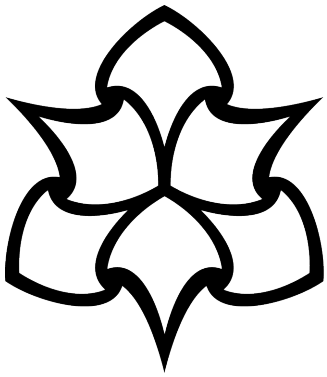

Journal Pre-proof

Deposition of Pt nanoparticles on TiO_2 by pulsed direct current magnetron sputtering for selective hydrogenation of vanillin to vanillyl alcohol

Boontida Pongthawornsakun, Palida Kaewsuanjik, Pongsakorn Kittipreechakun, Marina Ratova, Peter Kelly, Okorn Mekasuwandumrong, Piyasan Praserthdam, Joongjai Panpranot

PII: S0920-5861(19)30478-X

DOI: https://doi.org/10.1016/j.cattod.2019.08.045

Reference: CATTOD 12434

To appear in: *Catalysis Today*

Received Date: 18 February 2019

Revised Date: 28 July 2019

Accepted Date: 27 August 2019

Please cite this article as: Pongthawornsakun B, Kaewsuanjik P, Kittipreechakun P, Ratova M, Kelly P, Mekasuwandumrong O, Praserthdam P, Panpranot J, Deposition of Pt nanoparticles on TiO_2 by pulsed direct current magnetron sputtering for selective hydrogenation of vanillin to vanillyl alcohol, *Catalysis Today* (2019), doi: https://doi.org/10.1016/j.cattod.2019.08.045

Revised Manuscript

Deposition of Pt nanoparticles on TiO_2 by pulsed direct current magnetron sputtering for selective hydrogenation of vanillin to vanillyl alcohol

Boontida Pongthawornsakun[1], Palida Kaewsuanjik[1], Pongsakorn Kittipreechakun[1], Marina Ratova[2], Peter Kelly[2], Okorn Mekasuwandumrong[3], Piyasan Praserthdam[1], Joongjai Panpranot[1,*]

[1]*Center of Excellence on Catalysis and Catalytic Reaction Engineering, Department of Chemical Engineering, Faculty of Engineering, Chulalongkorn University, Bangkok 10330, Thailand*

[2]*Surface Engineering Group, Manchester Metropolitan University, Manchester, M1 5GD, UK*

[3]*Department of Chemical Engineering, Faculty of Engineering and Industrial Technology, Silpakorn University, Nakorn Pathom 73000, Thailand*

[*]Corresponding authors. Tel. 66-2218-6869 Fax. 66-2218-6877 E-mail: joongjai.p@chula.ac.th (J. Panpranot)

Date: July 28, 2019

Submitted to: *Catalysis Today (special issue: Proceedings of CCE-2019)*

Graphical abstract

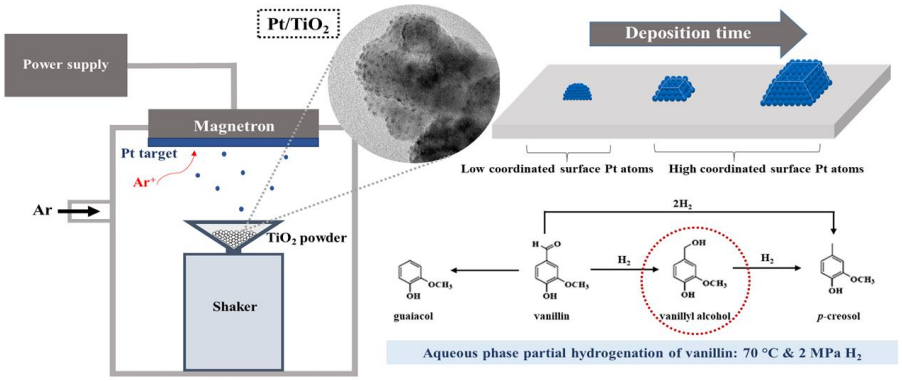

Highlights:

- Pt/TiO_2 were synthesized by pulsed direct magnetron sputtering deposition.
- Characteristics of Pt nanoparticles formed depended on deposition time.
- Small Pt with high-coordinated surface could be obtained via pulsed DC-MSD.
- Aqueous phase partial hydrogenation of vanillin was tested at 70 °C and 2MPa.
- Pt/TiO_2 prepared by pulsed DC-MSD was more effective than impregnation.

Abstract

Pulsed direct current magnetron sputtering (PDC-MSD) was employed for the deposition of Pt nanoparticles (ca. 0.1 wt.%) on anatase TiO_2 powder. According to the H_2-TPR, XPS, and TEM-EDX results, the characteristics and properties of the deposited nanoparticles depended on the deposition time. During the initial deposition stage (45-90 sec), low-coordinated small spherical Pt nanoparticles were formed. Prolonging the deposition time (135-180 sec), led to the formation of larger Pt nanoparticles, which strongly interacted with the TiO_2. The catalytic activities of the prepared Pt/TiO_2 with different deposition times in the aqueous phase partial hydrogenation of vanillin to vanillyl alcohol ranged as follows: Pt/TiO_2 MSD-45 < Pt/TiO_2 MSD-90 < Pt/TiO_2 MSD-180 < Pt/TiO_2 MSD-135, which was in good agreement with the atomic Pt/Ti ratio and coordinated surface Pt atoms on the catalyst surface. The high catalytic activity of Pt/TiO_2 MSD-135 was attributed to the presence of well-dispersed small Pt nanoparticles with more highly-coordinated Pt surface atoms deposited on the TiO_2 anatase.

PDC-MSD has been proven to be a more effective method for the preparation of supported metal catalysts, compared to those obtained by conventional impregnation technique.

Keywords: Pulsed DC magnetron sputtering; Selective hydrogenation; Vanillin; Vanillyl alcohol; Platinum

1. Introduction

Lignocellulosic biomass has been used largely for the production of pulp and paper via the Kraft process. Lignin waste can serve as a potential and abundant renewable phenolics class feedstock for sustainable production of chemicals and fuels. Vanillin (4-hydroxy-3-methoxybenzaldehyde) is emerging as one of the promising biomass-based platform chemicals, especially for applications in polymer chemistry. One of lignin derived aromatic diols, vanillyl alcohol (4-hydroxymethyl-2-methoxyphenol: HMP), which can be produced by the partial hydrogenation of the aldehyde group of vanillin (**Fig. 1**), is considered not only a valuable intermediate in the synthesis of novel flavorings and fragrances [1] but also a potential lignin-based building block for applications in high-performance thermosetting epoxy resins, such as the synthesis of renewable bisphenols and epoxy thermosets [2, 3]. Vanillyl alcohol can also be partially hydrodeoxygenated to *p*-creosol (2-methoxy-4-methylphenol: MMP), which is expected to be a potential future biofuel [4, 5].

Considering the hydrogenation of vanillin to vanillyl alcohol, various metals have been employed in the form of homogeneous and heterogeneous catalysts. Homogeneous catalysts used to produce the vanillyl alcohol have been typically based on Ru metals including $RuCl_2$/TPPTS [6], $RuCl_2(PPh_3)_3$ [7], and Ru-based Shvo [8]. In addition, heterogeneous catalysts have been investigated in this reaction by using different metals, such as Ru [9, 10], Rh [10], Au [10], Pt [10], Pd [5], Ni [11], and Ir [11]. According to literature, 5%Ru/C in the aqueous phase hydrogenation of vanillin under mild conditions (0.69 MPa and 318 K) showed 93% conversion and 59.4% selectivity to vanillyl alcohol within 1 h [9]. Whereas a yield of vanillyl alcohol production of more than 70% could be observed under extreme conditions (i.e., 3 MPa and 373 K) and longer reaction times [10, 11]. Pt-based catalysts have been reported to catalyze the

hydrogenation of vanillin (70% selectivity to vanillyl alcohol) with high Pt loadings (5%) under conditions of 3 MPa and 373 K for 3 h [10].

Pulsed direct current magnetron sputtering (PDC-MSD) is a well-known and developed deposition technique for coatings and thin film applications. This deposition technique has been widely used in the industry, because of its scalability, versatility, controllability, uniformity, high stability, repeatability, low environmental impact, and the high quality of the obtained coatings [12-15]. On a laboratory scale, PDC-MSD has recently been employed for the deposition of metal nanoparticles on solid surfaces or liquid supports, since the stabilizing and reducing agents typically needed for conventional techniques are not required, hence avoiding the contamination of precursors and/or solvents occurring on the surface of nanoparticles [12, 16]. However, the use of the magnetron sputtering technique to deposit metals onto powder substrate materials has only been investigated to a limited degree, for example, by the groups of Teixeira et al. [16-20] and Kelly et al. [12]. According to the literature, the primary and crucial advantage of applying the MSD technique to powder substrates, over conventional deposition techniques is the high amount of metal that can be deposited within short sputtering times [12, 16]. Moreover, this single stage technique not only provides the ability to control the amount of metal loading with precision, but maximizes the distribution of the metal across the greatest surface area of the powder, thus minimizing the usage of high priced metals, especially noble metals [17]. Nonetheless, the growth mechanisms of metal nanoparticles on the powder surface during PDC-MSD is not well known and understood.

In the present work, Pt catalysts supported on commercial TiO_2 anatase (Pt/TiO_2) were synthesized by using PDC-MSD with deposition times in the range of 45-180 seconds. The characteristics and properties of the Pt nanoparticles at different deposition times were studied and investigated by means of various characterization techniques. The catalytic performances of the Pt/TiO_2 catalysts were tested in the aqueous phase partial hydrogenation of vanillin to vanillyl alcohol under mild and green conditions (temperature of 70 ºC and H_2 pressure of 2 MPa using H_2O as the solvent). For comparison purposes, Pt/TiO_2 catalysts were also prepared by a conventional impregnation method with similar and higher Pt loadings (0.1 and 0.4 wt. %).

2. Experimental

2.1 Catalyst preparation

2.1.1 Catalyst preparation by pulse DC-MSD

Commercial TiO_2 anatase (Sigma-Aldrich) powder was used as the support for Pt deposition in this work. Platinum catalysts supported on titanium dioxides (Pt/TiO_2) were synthesized by using PDC-MSD with deposition times varying from 45 to 180 seconds, as described elsewhere [12]. A schematic diagram of the PDC-MSD system is shown in **Fig. 2**. The MSD system was employed in a sputter-down configuration consisting of a single 7.5 cm diameter type II unbalanced planar magnetron installed in the chamber lid as the magnetron sputtering source, along with the Pt target. The TiO_2 powder holder was placed underneath the magnetron and installed on a shaker mechanism, which allowed continuous powder mixing during the MSD process. The distance between the Pt target and the substrate was fixed at 5 cm. The magnetron sputtering source was powered by an Advanced Energy Pinnacle Plus power supply. The Pt target was sputtered at 250 W and 350 kHz with 50% duty cycle, corresponding to 1.4 μs pulse-off period. Sputtering took place under an Ar atmosphere at a working pressure of approximately 2.6 Pa. For each run, 2 g of commercial TiO_2 anatase powder was located in the substrate holder and treated for different sputtering times (45-180 seconds). The obtained samples after Pt deposition via this technique are denoted as "MSD" followed by deposition time (in sec).

2.1.2 Catalyst preparation by conventional impregnation method

The Pt/TiO_2 (0.1 and 0.4 wt.% Pt) catalysts were prepared by the incipient wetness impregnation method. The commercial TiO_2 anatase (Sigma-Aldrich) powders were impregnated with an aqueous solution of chloroplatinic acid (H_2PtCl_6, Aldrich) as the Pt precursor. After that, the obtained catalysts were dried in an oven at 100 ºC overnight, and calcined in air at 400 ºC for 4 h. The Pt/TiO_2 catalysts prepared by incipient wetness impregnation method are denoted as "IMP".

2.2 Catalyst characterization

The samples were analysed by X-ray diffraction (XRD) and the XRD patterns were recorded by using a Bruker D8 Advance X-ray diffractometer with Ni-filtered CuK_α radiation over the scanning range of 20 to 80º 2θ. The actual amount of Pt deposited on the TiO_2 supports

by each technique were analyzed using an ICP-OES technique. To determine the specific surface areas, pore volumes and average pore diameters, N_2 physisorption was conducted by using a Micrometrics ASAP 2020 instrument with the Brunauer–Emmett–Teller (BET) method. The TEM micrographs and EDX results of the catalysts were detected by using a JEOL (JEM-2010) transmission electron microscope operated at 200 kV and equipped with a LaB_6 electron beam source and an energy dispersive x-ray spectrometry (EDX). The scanning electron microscopy with energy dispersive X-ray analysis (SEM-EDX) was performed by using a Hitachi S-3400N coupled with AMETEK EDAX (APOLLO X). The reducibility of the catalysts as a function of temperature was determined by using the H_2-temperature programmed reduction technique which was carried out on a Micromeritics ChemiSorb 2750 with ChemiSoft TPx software. The samples were pretreated under a flow of N_2 (25 cm^3/min) at 200 ºC for 1 h. After cooling down to room temperature, each sample was exposed to a mixture of 10% H_2 in Ar (25 cm^3/min) with a temperature ramp of 10 ºC/min from room temperature to 800 ºC. X-ray photoelectron spectroscopy (XPS) was conducted on a Kratos AMICUS X-ray photoelectron spectrometer with using MgK_α as the X-ray radiation source to determine the surface properties. The XPS spectra of C 1s line was set at binding energy of 285.0 eV as the internal standard.

2.3 Catalytic reaction study

The catalytic performances of the Pt/TiO_2 catalysts were tested in the liquid-phase selective hydrogenation of vanillin to vanillyl alcohol under mild and green conditions. Approximately 0.05 g of catalyst was dispersed into the reactant mixture of 0.05 g vanillin and 10 ml H_2O in a 100 cm^3 stainless steel autoclave reactor (JASCO, Tokyo, Japan). The selective hydrogenation was carried out at a temperature of 70 ºC and H_2 pressure of 2 MPa for 2 h. Afterwards, the autoclave reactor was quickly cooled down with ice-cold water and then depressurized. The catalyst was filtered from the liquid product and then the liquid product was collected and analyzed by high-performance liquid chromatography (HPLC). For the catalyst prepared by the conventional impregnation method, the catalyst was reduced with hydrogen (30 cm^3/min) at 500 ºC for 2 h prior to the reaction test.

The liquid product analysis was carried out on a HPLC instrument. The reactant and products, consisting of vanillin, vanillyl alcohol, p-creosol, and guaiacol, were separately detected by a ZORBAX SB-C18 column (4.6 mm inner diameter x 150 mm length; Agilent) and

a UV detector at 230 nm. The mobile phase was composed of acetronitrile (HPLC grade) and water (HPLC grade) with a volumetric ratio of 60:40 and the total flow rate was set at 0.3 ml/min. The column temperature was kept at room temperature.

3. Results and discussion

3.1 Catalyst characteristics

The amounts of Pt deposited onto the anatase samples by PDC-MSD were analyzed by using the ICP technique and the elemental results are shown in **Table 1**. The actual Pt loading increased marginally from 0.08 wt.% and reached a steady state at ca. 0.12 wt.% as the deposition time was increased from 45 to 180 sec. The average Pt deposition rate decreased with increasing deposition time. It is possible that target poisoning was occurred during the sputtering process. Thus, only ca. 0.1 wt.% Pt was deposited on the commercial TiO_2 anatase support under such conditions.

The N_2 adsorption-desorption isotherms of the anatase TiO_2 support before Pt and after Pt deposition by PDC-MSD are shown in **Fig. 3**. According to the Brunauer-Deming-Deming-Teller (BDDT) classification of sorption isotherms, the commercial TiO_2 anatase support showed a type IV isotherm with a distinct hysteresis loop at moderate to high relative pressure in the range of 0.4-1.0, describing the presence of a large number of mesopores in the TiO_2 support [21]. In addition, the hysteresis loop observed on the TiO_2 support was type H3 due to the absence of any limiting adsorption at high P/P_0, indicating slit shaped pores. After the Pt deposition, the characteristics of sorption isotherms were altered to the unusual hysteresis loop with two inflection points, suggesting bimodal porosity. The initial inflection was found to be at higher relative pressures (from 0.4 for the TiO_2 support to 0.5 after Pt deposition). The BET specific surface area, pore volume, and average pore diameter of all samples are presented in **Table 2**. The decrease in BET specific surface area, pore volume, and average pore diameter of

the Pt/TiO_2 catalysts compared to the bare TiO_2 anatase support were due to the Pt deposition on the pores of TiO_2 support, resulting in the formation of pore blockages and new pore structures.

The reduction behaviors of the Pt-based catalysts were studied by the H_2-TPR technique and the H_2-TPR profiles of the TiO_2 anatase support and the Pt/TiO_2 catalysts prepared by PDC-MSD and conventional impregnation methods are shown in **Fig. 4**. According to the H_2-TPR profile of the TiO_2 anatase support, the partial reduction of the bare TiO_2 support itself was found to be at high temperature (500-600 ºC). The Pt/TiO_2 catalysts prepared by conventional impregnation showed three reduction peaks at 90-120 ºC, 270-350 ºC, and 500-650 ºC. The first reduction peak was assigned to the reduction of Pt oxides to Pt metal [22, 23]; this peak was clearly observed on the catalyst with a large amount of Pt loading. In addition, the reduction peak at 270-350 ºC could be attributed to the reduction of Pt species interacting with the TiO_2 support in the form of Pt-TiO_x interface sites [22]. The reduction peak at temperatures above 500 ºC was associated with the reduction of surface capping oxygen of the TiO_2 support or the partial reduction of the TiO_2 support itself [22, 23].

Considering the reduction behaviors of the Pt/TiO_2 catalysts prepared by PDC-MSD, it is surprising that the presence of a significant negative TPR peak was found on these catalysts, indicating hydrogen release instead of H_2 consumption, due probably to the decomposition of Pt hydride (PtH_x) formed earlier with hydrogen. Meanwhile, the absence of any significant detectable hydrogen consumption (as indicated by a positive TPR peak) in advance of hydrogen release (as indicated by a negative TPR peak) proved the ability of Pt to absorb hydrogen, forming PtH_x at room temperature. Comparing the hydrogen absorption on Pt and Pd, the ability to absorb and desorb hydrogen of Pd black would occur at ambient temperature but the hydrogen absorbed on the Pt black surface could not be released by evacuation under ambient conditions since the interaction between Pt and hydrogen is very strong [24]. Thus, it is reasonable to attribute the higher temperature for PtH_x decomposition found in this work, as compared to PdH_x decomposition occurring at less than 100 ºC [25]. According to literature, the formation of a hydride-like phase is favorable only for small particles sizes [24, 26, 27]. The presence of PtH_x has been reported to occur on the catalysts having lower Pt amounts and finer particles, whereas the behavior of larger Pt particles formed in the catalysts with high Pt amounts would be stable against transformation into PtH_x [27]. Hence, it could be suggested that small Pt nanoparticles were formed on the TiO_2 supports upon PDC-MSD.

XPS characterization was used to detect surface properties such as chemical composition and the electronic structure of each chemical species on the catalyst surface. The XPS spectra of Pt 4f could be fitted and resolved into 3 species with 3.35 eV spin-orbit splitting and FWHM < 2 consisting of Pt metal, PtO, and PtO_2 species (as shown in **Fig. 5**). According to literature, the typical binding energies of Pt in the form of Pt metal, PtO, and PtO_2 species appears at ca. 71, 72.4, 74.9 eV, respectively [28-32]. Considering the Pt/TiO_2 prepared by PDC-MSD, the shift in XPS peaks due to Pt metal towards lower binding energy, as compared to the value reported in the references, could be attributed to several factors. One of the factors was due to the electron transfer from the TiO_2 to the metallic Pt nanoparticles [29]. Nevertheless, the shape of the particles could be accounted as a critical factor in the negative shift [33]. Radnik et al. reported that for the initial state effects on Au nanoparticles supported on TiO_2 the Au nanoparticles that were more spherical exhibited shifts in Au 4f binding energy towards a lower value, as compared to Au metal, because the spherical particles would have less coordinated surface atoms, thus reducing their binding energy as compared to nanoparticles with large faces [34]. Furthermore, the initial stages of Cu growth on Al_2O_3 films has been studied and reported that the coverage-dependent shifting in Cu 2p during Cu growth consisted of the initial state and final state contributions [35, 36]. At very low Cu coverage, the initial-state was found to contribute to the negative shifts of Cu clusters formed, indicating a reduced average coordination number of Cu atoms in clusters. However, this initial state effect diminished rapidly when the Cu coverage increased and then the final state effect would rather contribute and affect the shifting in binding energy towards positive values. Regarding this effect, the final state Coulomb energy is roughly proportional to 1/r where r is the average radius of metal clusters, so the final state effect is very sensitive to the cluster size. Thus, the average size of Cu clusters increases as Cu overlayers grow and the Cu 2p binding energy was found to decrease. In other words, the Cu 2p binding energy was found to be larger on the smaller Cu cluster size at the same Cu coverage. The positive shifting in binding energy of core and valence electrons with decreasing the particle size has been reported in various metals such as Au, Cu, Ag, Pd, Ni, and Pt [30, 37-39].

According to the studies reported earlier about the relation between the binding energy and the growth of nanoparticles and/or clusters, it could be described as follows: more negative shifts in Pt 4f for the Pt/TiO_2 MSD-45 coating was due to a larger initial state effect, indicating

the presence of more low-coordinated Pt atoms in these nanoparticles and/or clusters deposited. It might be ascribed to a smaller average size of the Pt nanoparticles and/or clusters with a more spherical shape formed within this deposition time. However, the initial state effect was found to be diminished until a deposition time of 135 seconds and the shift in Pt 4f binding energy was related to the size of the Pt nanoparticles and/or clusters according to the final state effect. Thus, the Pt/TiO_2 MSD-135 coating showed a large number of smaller Pt nanoparticles and/or clusters with higher Pt 4f binding energy as compared to Pt/TiO_2 MSD-180. With longer deposition time up to 180 seconds, the Pt 4f binding energy shifted to lower values because of the larger size of the Pt nanoparticles and/or clusters formed during PDC-MSD. Interestingly, a large shifting in Pt 4f binding energy towards lower and negative values was observed for Pt/TiO_2 MSD-180 and the origin of this shift is thereby probably due to synergistic contributions between the final state effect and the interaction between Pt and TiO_2 in which the charges transferred from the TiO_2 to the metallic Pt. This negative shift results was also reported on Au nanoparticles deposited on Al_2O_3 using the magnetron sputtering technique [33].

From the composition of each Pt species as presented in **Table 3**, all the Pt/TiO_2 catalysts prepared by PDC-MSD showed the majority of Pt metal species together with Pt oxides. The atomic ratios of Pt/Ti at the catalyst surface were found to increase with deposition times, except the Pt/TiO_2 MSD-180. The lower Pt/Ti atomic ratio on the Pt/TiO_2 MSD-180 was probably due to the growth of larger Pt nanoparticles. In addition, the XPS spectra of Pt 4f on the Pt/TiO_2 catalyst prepared by conventional impregnation with similar Pt loading (0.1%Pt/TiO_2 IMP) was not clearly detected. However, this spectra could be detected on the Pt/TiO_2 catalyst prepared by conventional impregnation with high Pt loading as observed on sample 0.4%Pt/TiO_2 IMP and it was found that no Pt metal species was formed upon conventional impregnation.

According to **Fig. 6**, the binding energy of Ti 2p for the bare TiO_2 anatase was mainly located at 458.8 eV, which was assigned to the presence of Ti^{4+} in the TiO_2 support. After Pt deposition by pulsed sputtering, this XPS peak of Ti 2p slightly shifted to higher binding energy as compared to the bare support. This shift could be attributed to the electron transfer from the TiO_2 to metallic Pt due to the larger electronegativity of Pt as compared to Ti^{4+}. In contrast, the reverse shift of XPS Ti 2p peaks towards lower binding energy was found on the Pt/TiO_2 catalysts prepared by conventional impregnation. Similar to Choi et al. [40], the shift of XPS Ti

2p peaks towards higher binding energy for the V-TiO_2 catalyst as compared to the TiO_2 anatase was found to be restored upon Pt impregnation —the binding energy of Ti 2p was reversely decreased after Pt impregnation on the V-TiO_2 catalyst. Moreover, the Pt states observed on the Pt/TiO_2 prepared by conventional impregnation exhibited the Pt oxides species consisted of Pt^{2+} and Pt^{4+} species. It might be possible that the oxygen contained in the Pt oxides promoted the electron transfer towards the TiO_2 support, thus decreasing the binding energy of Ti 2p.

Considering the TiO_2 support, the XPS O 1s peaks were mainly exhibited at 530.1 eV, representing the lattice oxygen in the TiO_2 support as presented in **Fig. 7**. In addition, the peaks appearing at 531.6 eV were attributed to the hydroxyl radicals (OH^-) [41, 42] and/or surface oxygen [43, 44]. The higher binding energy of surface oxygen compared to the lattice oxygen in bulk was due to the open bonds [44]. Considering the binding energy of lattice oxygen after Pt deposition by PDC-MSD, this XPS peaks shifted towards higher values, suggesting an interaction between Pt metal and TiO_2 support. This evidence for the interaction between Pt and TiO_2 has been reported on the Pt/TiO_2 prepared via precipitation [45]. Meanwhile, the peak shifting of the lattice oxygen was absence on the Pt impregnation. For the surface oxygen, the XPS peaks still remained at ca. 531.6 eV on both of catalyst types; after Pt deposition by PDC-MSD and after Pt impregnation. The O 1s peaks due to adsorbed water (O_{H2O}) were detected at high binding energy ca. 533.3-533.7 eV [43, 46]. Interestingly, the XPS O 1s peaks on the catalysts prepared by impregnation could be deconvoluted into 4 peaks in which another peak was found at higher binding energy ca. 532.6 eV, probably due to the formation of Pt oxides. The high binding energy of this peak seemed to be reasonable for the decrease in binding energy of Ti 2p upon Pt impregnation. Saputera et al. reported that more O^-_{ads} detected on the XPS results could be accounted for increasing in Pt oxides in the form of PtO_{ads} [47].

The TEM micrographs of the Pt/TiO_2 catalysts prepared by PDC-MSD at 135 and 180 seconds are shown in **Fig. 8**. The state of Pt dispersion on the TiO_2 support can be seen from these TEM images. The Pt deposition using the PDC-MSD technique has provided highly dispersed small Pt nanoparticles on the TiO_2 support and uniform metal particle distribution especially for sample Pt/TiO_2 MSD-135. Moreover, the distribution of Pt on TiO_2 support was also confirmed via the SEM-EDX analysis (as shown in **Fig. S2** to **Fig. S5** of the Supporting Information). However, the homogeneity of the metal dispersion could be further improved by

optimizing the operational conditions, for instance by lowering the sputtering power and by adopting longer deposition times, or a higher powder shaking frequency during metal sputtering [12]. The Pt particle size observed on Pt/TiO_2 MSD-180 (ca. 1.5-2.5 nm) was slightly larger than that of Pt/TiO_2 MSD-135 (ca. 0.9-1.4 nm) which corresponded to the shifting in Pt 4f binding energy and decrease in Pt/Ti ratio. The EDX analysis confirmed the presence of Pt nanoparticles deposited on the TiO_2 support.

In the sputtering process, ions generated in a plasma strike a target surface and remove target atoms via a momentum exchange process [48, 49]. In this work, the sputtered Pt target atoms may then deposit on the surface of the TiO_2 substrate as adatoms. These Pt adatoms will subsequently aggregate/agglomerate and grow in size, thus forming Pt metallic nanoparticles [16, 50]. According to our results, the deposition time played a crucial role on the characteristics and properties of the Pt nanoparticles and/or clusters deposited on the TiO_2 support. A schematic of the formation of Pt nanoparticles during PDC MSD is proposed as illustrated in **Fig. 9**. During deposition times between 45-90 seconds, the Pt atoms/clusters were sputtered from the sputtering target and then grow as very small Pt nanoparticles with more spherical and low-coordinated surfaces as shown by the more negative shift in the Pt 4f binding energy relative to Pt metal. In addition, at deposition times of 135 seconds a large number of small Pt nanoparticles with more highly-coordinated surface atoms (larger faces) were deposited on the TiO_2 as observed at high atomic Pt/Ti ratios at the catalyst surface and the final state contribution in the Pt 4f binding energy (positive shift). Then, the growth step of the Pt nanoparticles still proceeded and formed the larger Pt nanoparticles observed, which strongly interacted with the TiO_2 supports.

3.2 Catalytic reaction study

The catalytic activities of the prepared catalysts were evaluated in an aqueous phase partial hydrogenation of vanillin to vanillyl alcohol under mild reaction conditions (temperature of 70 ºC and H_2 pressure of 2 MPa) and the results are summarized in **Table 4**. The use of H_2O as a desirable green solvent is beneficial to the process in the terms of safety, cost, and environmental impacts. Moreover, using H_2O instead of an organic solvent, such as ethanol,

could prevent the loss of vanillyl alcohol due to the reaction with methanol forming vanillyl ethyl ether [51].

Considering the Pt/TiO_2 catalysts prepared by pulsed magnetron sputtering without the reduction step, the conversion of vanillin ranged in the order of Pt/TiO_2 MSD-45 < Pt/TiO_2 MSD-90 < Pt/TiO_2 MSD-180 < Pt/TiO_2 MSD-135 catalysts, which was found to correlate to the atomic ratios of Pt/Ti on the catalyst surfaces. Moreover, the low activities of small Pt nanoparticles observed on Pt/TiO_2 MSD-45 and Pt/TiO_2 MSD-90 could be attributed to a larger fraction of low-coordinated sites, as compared to Pt deposition for longer times. The size effect of Pt has been investigated in the selective hydrogenation of cinnamaldehyde and it was reported that small Pt nanoparticles showed poor selectivity to cinnamyl alcohol because of the presence of more low coordination sites on small sized Pt nanoparticles [52]. The low coordination Pt sites are well-known to have a strong binding to C=C bonds, thus favoring C=C hydrogenation and decreasing C=O hydrogenation [52, 53]. The low coordination Pt sites were found to be more intense on small Pt nanoparticles, whereas larger sized Pt nanoparticles showed relatively fewer low coordination sites, leading to higher C=O hydrogenation [52]. Thus, the suitable characteristics of Pt nanoparticles deposited on TiO_2 anatase powder by PDC-MSD should be a large number of well-dispersed and small Pt nanoparticles with more high-coordinated Pt surface atoms, which depended on the deposition time under the conditions tested here.

In addition, the Pt/TiO_2 catalysts prepared by the conventional impregnation method with similar and higher Pt loadings were also compared under similar reaction conditions. It was found that the Pt/TiO_2 MSD-135 exhibited higher activity in the hydrogenation of vanillin, as compared to the 0.1%Pt/TiO_2 IMP, due to higher amount of metallic Pt nanoparticles on the catalyst surface and a uniform small Pt nanoparticle dispersion. Moreover, the Pt/TiO_2 MSD-135 sample seemed to be interesting and to be more effective than 0.4%Pt/TiO_2 IMP, because of the 4 times lower Pt loading and the prompt catalyst application in reaction without a reduction step.

The effect of a reduction step on the Pt/TiO_2 catalysts prepared by PDC-MSD was further investigated for the Pt/TiO_2 MSD-135 and Pt/TiO_2 MSD-180 catalysts. The catalytic activities of the Pt/TiO_2 MSD-135 and Pt/TiO_2 MSD-180 catalysts after reduction at 500 ºC were found to be lower than those without a reduction step. According to the XPS results, after the reduction step the atomic ratios of Pt/Ti at the catalyst surface after reduction at high temperature were found to

decrease (Pt/Ti ratios: 0.020 and 0.006 for Pt/TiO_2 MSD-135 R500 and Pt/TiO_2 MSD-180 R500, respectively) due probably to the migration of TiO_x species onto the Pt nanoparticles, thus leading to lower catalytic activities. Thus, the reduction step prior to reaction was unnecessary for the catalysts prepared by PDC-MSD. For the product distribution, all the Pt catalysts showed relatively high selectivity to vanillyl alcohol up to 98%. Only little *p*-creosol was formed as the by-product.

The reusability and stability of the Pt/TiO_2 MSD-135 was studied in the 2nd cycle reaction without regeneration. The recycle procedures used for the catalyst synthesized by PDC-MSD are described as follows: the spent catalyst was recovered by filtering them from the solution, washing with DI water for 3-5 times, and then drying the catalyst in air. The Pt/TiO_2 MSD-135 catalyst was still found to be effective for the 2nd cycle reaction in terms of catalytic performances and high activity without regeneration and reduction steps.

According to the literature, Pt-based catalysts have not been investigated in the vanillin hydrogenation to much of a degree. Besides the conversion and selectivity, the performance of the catalyst should be concerned in the term of ability of one active site to catalyze and convert the reactant, also known as TON and TOF values. Comparing the current work with those reported in the literature as shown in **Table 5**, it was found that the Pt/TiO_2 catalysts prepared by using PDC-MSD were very active in the hydrogenation of vanillin. Higher TON and TOF values observed on the Pt/TiO_2 MSD-180, as compared to the Pt/TiO_2 MSD-135, were due to larger Pt particles, thus promoting C=O hydrogenation. In addition, the TON and TOF values of the Pt/TiO_2 prepared by impregnation were lower than the Pt/TiO_2 prepared by PDC-MSD. The commercial 5wt.%Pt/C catalysts, which have been reported previously in the other works, seemed to be less active according to the lower values of TON and TOF. Thus, the superior performances and efficiency of the Pt/TiO_2 catalysts prepared by PDC-MSD could be confirmed as presented in this work.

4. Conclusions

Pt catalysts supported on commercial TiO_2 anatase powders were synthesized by using pulsed magnetron sputtering with deposition times in the range of 45-180 seconds. The actual Pt loadings under such conditions were ca. 0.1 wt.%. According to the H_2-TPR, XPS, and TEM-

EDX results, the characteristics and properties of Pt nanoparticles formed via PDC-MSD were found to depend on the deposition time. During shorter deposition times between 45-90 seconds, very small Pt nanoparticles with more spherical and low-coordinated surfaces were formed. In addition, a large of small Pt nanoparticles with more high-coordinated surface atoms were be obtained at a deposition time of 135 seconds. After that, the growth step of Pt nanoparticles still proceeded forming larger Pt nanoparticles which strongly interacted with the TiO_2 supports. The catalytic activities of the Pt/TiO_2 MSD under different deposition times in the selective hydrogenation of vanillin to vanillyl alcohol under mild and green conditions were ranging as follows: Pt/TiO_2 MSD-45 < Pt/TiO_2 MSD-90 < Pt/TiO_2 MSD-180 < Pt/TiO_2 MSD-135 catalysts, which was in good agreement with the atomic Pt/Ti ratio on the catalyst surface and the presence of coordinated surface Pt atoms. A large number of well-dispersed and small Pt nanoparticles with more high-coordinated Pt surface atoms deposited on TiO_2 anatase powder by PDC-MSD was found to be suitable for the selective hydrogenation of vanillin and to be more effective than those prepared by conventional impregnation in terms of catalytic performances and high activity without a reduction step.

Acknowledgements

The authors also would like to acknowledge the financial supports from the Rachadapisek Sompote Fund for the Postdoctoral Fellowship, Chulalongkorn University for B.P., the Thailand Research Fund (BRG6180001-Joongjai Panpranot), CAT-REAC industrial project (RDG6150012) and Newton Mobility Grants.

References

[1] Reduction of Vanillin to Vanillyl Alcohol, http://www1.udel.edu/chem/CHEM322/Handouts/vanillin_reduction.
[2] E. Hernandez, Synthesis and characterization of vanillyl alcohol based thermosetting epoxy resins, Department of Chemical Engineering, Rowan University, 2015, pp. 120.
[3] J.F. Stanzione, Vanillyl Alcohol: A Renewable Epoxy Resin Building Block, 2015.
[4] C. Liao, X. Liu, Y. Ren, D. Gong, Z. Zhang, Catalytic deoxygenation of vanillin over layered double hydroxide supported Pd catalyst, J. Ind. Eng. Chem. 68 (2018) 380-386.
[5] H. Jiang, X. Yu, X. Peng, H. Zhang, R. Nie, X. Lu, D. Zhou, Q. Xia, Efficient aqueous hydrodeoxygenation of vanillin over a mesoporous carbon nitride-modified Pd nanocatalyst, RSC Adv. 6 (2016) 69045-69051.
[6] F.H. Mahfud, S. Bussemaker, B.J. Kooi, G.H. Ten Brink, H.J. Heeres, The application of water-soluble ruthenium catalysts for the hydrogenation of the dichloromethane soluble fraction of fast pyrolysis oil and related model compounds in a two phase aqueous–organic system, J. Mol. Catal. A Chem. 277 (2007) 127-136.
[7] F. Huang, W. Li, Q. Lu, X. Zhu, Homogeneous Catalytic Hydrogenation of Bio-Oil and Related Model Aldehydes with $RuCl_2(PPh_3)_3$, Chem. Eng. Technol. 33 (2010) 2082-2088.
[8] L. Busetto, D. Fabbri, R. Mazzoni, M. Salmi, C. Torri, V. Zanotti, Application of the Shvo catalyst in homogeneous hydrogenation of bio-oil obtained from pyrolysis of white poplar: New mild upgrading conditions, Fuel 90 (2011) 1197-1207.
[9] A.B. Bindwal, P.D. Vaidya, Reaction Kinetics of Vanillin Hydrogenation in Aqueous Solutions Using a Ru/C Catalyst, Energy Fuels 28 (2014) 3357-3362.
[10] J.L. Santos, M. Alda-Onggar, V. Fedorov, M. Peurla, K. Eränen, P. Mäki-Arvela, M.Á. Centeno, D.Y. Murzin, Hydrodeoxygenation of vanillin over carbon supported metal catalysts, Appl. Catal. A Gen. 561 (2018) 137-149.
[11] M. Alda-Onggar, P. Mäki-Arvela, A. Aho, I.L. Simakova, D.Y. Murzin, Hydrodeoxygenation of phenolic model compounds over zirconia supported Ir and Ni-catalysts, React. Kinet. Mech. Catal. (2018).
[12] M. Bernareggi, G.L. Chiarello, G. West, M. Ratova, A.M. Ferretti, P. Kelly, E. Selli, Cu and Pt clusters deposition on TiO_2 powders by DC magnetron sputtering for photocatalytic hydrogen production, Catal. Today (2018).
[13] A.S. Reddy, N.M. Figueiredo, A. Cavaleiro, Pulsed direct current magnetron sputtered nanocrystalline tin oxide films, Appl. Surf. Sci. 258 (2012) 8902-8907.
[14] J. O'Brien, P.J. Kelly, Characterisation studies of the pulsed dual cathode magnetron sputtering process for oxide films, Surf. Coat. Technol. 142-144 (2001) 621-627.
[15] W.M. Posadowski, Pulsed magnetron sputtering of reactive compounds, Thin Solid Films 343-344 (1999) 85-89.
[16] R.V. Gonçalves, R. Wojcieszak, H. Wender, C. Sato B. Dias, L.L.R. Vono, D. Eberhardt, S.R. Teixeira, L.M. Rossi, Easy Access to Metallic Copper Nanoparticles with High Activity and Stability for CO Oxidation, ACS Appl. Mater. Interfaces 7 (2015) 7987-7994.
[17] M.P. Languer, F.R. Scheffer, A.F. Feil, D.L. Baptista, P. Migowski, G.J. Machado, D.P. de Moraes, J. Dupont, S.R. Teixeira, D.E. Weibel, Photo-induced reforming of alcohols with improved hydrogen apparent quantum yield on TiO_2 nanotubes loaded with ultra-small Pt nanoparticles, Int. J. Hydrogen Energy 38 (2013) 14440-14450.

[18] R.V. Gonçalves, R. Wojcieszak, P.M. Uberman, D. Eberhardt, E. Teixeira-Neto, S.R. Teixeira, L.M. Rossi, Catalytic abatement of CO over highly stable Pt supported on Ta_2O_5 nanotubes, Catal. Commun. 48 (2014) 50-54.
[19] L. Luza, A. Gual, D. Eberhardt, S.R. Teixeira, S.S.X. Chiaro, J. Dupont, "Imprinting" Catalytically Active Pd Nanoparticles onto Ionic-Liquid-Modified Al_2O_3 Supports, ChemCatChem 5 (2013) 2471-2478.
[20] R. Bussamara, D. Eberhardt, A.F. Feil, P. Migowski, H. Wender, D.P. de Moraes, G. Machado, R.M. Papaléo, S.R. Teixeira, J. Dupont, Sputtering deposition of magnetic Ni nanoparticles directly onto an enzyme surface: a novel method to obtain a magnetic biocatalyst, Chem. Commun. 49 (2013) 1273-1275.
[21] Y. Zhang, L. Chen, S. Mao, Z. Sun, Y. Song, R. Zhao, Fabrication of porous graphene electrodes via CO_2 activation for the enhancement of capacitive deionization, J. Colloid Interface Sci. 536 (2019) 252-260.
[22] S. Pisduangdaw, O. Mekasuwandumrong, H. Yoshida, S.-I. Fujita, M. Arai, J. Panpranot, Flame-made Pt/TiO_2 catalysts for the liquid-phase selective hydrogenation of 3-nitrostyrene, Appl. Catal. A Gen. 490 (2015) 193-200.
[23] C. Zhang, H. He, K.-i. Tanaka, Catalytic performance and mechanism of a Pt/TiO_2 catalyst for the oxidation of formaldehyde at room temperature, Appl. Catal. B Environ. 65 (2006) 37-43.
[24] M. Yamauchi, H. Kobayashi, H. Kitagawa, Hydrogen Storage Mediated by Pd and Pt Nanoparticles, ChemPhysChem 10 (2009) 2566-2576.
[25] B. Pongthawornsakun, O. Mekasuwandumrong, S. Prakash, E. Ehret, F.J.C. Santos Aires, J. Panpranot, Effect of reduction temperature on the characteristics and catalytic properties of TiO_2 supported AuPd alloy particles prepared by one-step flame spray pyrolysis in the selective hydrogenation of 1-heptyne, Appl. Catal. A Gen. 506 (2015) 278-287.
[26] K.A. Stoerzinger, M. Favaro, P.N. Ross, J. Yano, Z. Liu, Z. Hussain, E.J. Crumlin, Probing the Surface of Platinum during the Hydrogen Evolution Reaction in Alkaline Electrolyte, J. Phys. Chem. B 122 (2018) 864-870.
[27] A.V. Kalinkin, A.V. Pashis, V.I. Bukhtiyarov, X-ray photoelectron study of the interaction of H_2 and H_2+O_2 mixtures on the Pt/MoO_3 model catalyst, J. Struct. Chem. 49 (2008) 255-260.
[28] F. Şen, G. Gökağaç, Different Sized Platinum Nanoparticles Supported on Carbon: An XPS Study on These Methanol Oxidation Catalysts, J. Phys. Chem. C 111 (2007) 5715-5720.
[29] J. Papavasiliou, A. Paxinou, G. Słowik, S. Neophytides, G. Avgouropoulos, Steam Reforming of Methanol over Nanostructured Pt/TiO_2 and Pt/CeO_2 Catalysts for Fuel Cell Applications, Catalysts 8 (2018) 544.
[30] L.-J. Chen, H. Ma, K.-C. Chen, W. Fan, H.-R. Cha, Y.-I. Lee, D.-J. Qian, J. Hao, H.-G. Liu, Synthesis and assembly of catalytically active platinum-doped polymer nanocomposites at the liquid/liquid interface, Colloids Surf. A 386 (2011) 141-150.
[31] Z. Jiang, J. Li, W. Liao, G. Fan, H. Yu, L. Chen, Z. Su, Synthesis and Characterization of the Optical Properties of $Pt\text{-}TiO_2$ Nanotubes, J. Nanomater. 2017 (2017) 9.
[32] J. Zhang, M. Zhang, Z. Jin, J. Wang, Z. Zhang, Study of high-temperature hydrogen reduced Pt^0/TiO_2 by X-ray photoelectron spectroscopy combined with argon ion sputtering—Diffusion-encapsulation effect in relation to strong metal–support interaction, Appl. Surf. Sci. 258 (2012) 3991-3999.
[33] G.M. Veith, A.R. Lupini, S.J. Pennycook, G.W. Ownby, N.J. Dudney, Nanoparticles of gold on $\gamma\text{-}Al_2O_3$ produced by dc magnetron sputtering, J. Catal. 231 (2005) 151-158.

[34] J. Radnik, C. Mohr, P. Claus, On the origin of binding energy shifts of core levels of supported gold nanoparticles and dependence of pretreatment and material synthesis, Phys. Chem. Chem. Phys. 5 (2003) 172-177.
[35] Y. Wu, E. Garfunkel, T.E. Madey, Initial stages of Cu growth on ordered Al_2O_3 ultrathin films, J. Vac. Sci. Technol. A 14 (1996) 1662-1667.
[36] C.R. Henry, Surface studies of supported model catalysts, Surf. Sci. Rep. 31 (1998) 231-325.
[37] I. Aruna, B.R. Mehta, L.K. Malhotra, S.M. Shivaprasad, Size dependence of core and valence binding energies in Pd nanoparticles: Interplay of quantum confinement and coordination reduction, J. Appl. Phys. 104 (2008) 064308.
[38] F.F. Schweinberger, Catalysis with Supported Size-selected Pt Clusters: Fundamental UHV and Applied Ambient Experiments, Catalysis Research Center, Department of Chemistry, Technische Universität München, Garching, Germany, Springer, Cham, 2014, pp. 222.
[39] Y. Watanabe, X. Wu, H. Hirata, N. Isomura, Size-dependent catalytic activity and geometries of size-selected Pt clusters on TiO_2(110) surfaces, Catal. Sci. Technol. 1 (2011) 1490-1495.
[40] Hyung-Joo Choi, Jun-Sik Kim, Misook Kang, Photodecomposition of Concentrated Ammonia over Nanometer-sized TiO_2, V-TiO_2, and Pt/V-TiO_2 Photocatalysts, Bull. Korean Chem. Soc. 28 (2007) 581-588.
[41] A. Wiatrowski, M. Mazur, A. Obstarczyk, D. Wojcieszak, D. Kaczmarek, J. Morgiel, D. Gibson, Comparison of the Physicochemical Properties of TiO_2 Thin Films Obtained by Magnetron Sputtering with Continuous and Pulsed Gas Flow, Coatings 8 (2018) 412.
[42] B. Xin, L. Jing, Z. Ren, B. Wang, H. Fu, Effects of Simultaneously Doped and Deposited Ag on the Photocatalytic Activity and Surface States of TiO_2, J. Phys. Chem. B 109 (2005) 2805-2809.
[43] B. Pongthawornsakun, S. Phatyenchuen, J. Panpranot, P. Praserthdam, The low temperature selective oxidation of H_2S to elemental sulfur on TiO_2 supported V_2O_5 catalysts, J. Environ. Chem. Eng. 6 (2018) 1414-1423.
[44] P. Georgios, S.M. Wolfgang, X-Ray Photoelectron Spectroscopy of Anatase-TiO_2 Coated Carbon Nanotubes, Solid State Phenom. 162 (2010) 163-177.
[45] L. Yu, Y. Shao, D. Li, Direct combination of hydrogen evolution from water and methane conversion in a photocatalytic system over Pt/TiO_2, Appl. Catal. B Environ. 204 (2017) 216-223.
[46] M. Peuckert, XPS investigation of surface oxidation layers on a platinum electrode in alkaline solution, Electrochim. Acta 29 (1984) 1315-1320.
[47] W.H. Saputera, J. Scott, N. Ganda, G.K.C. Low, R. Amal, The role of adsorbed oxygen in formic acid oxidation by Pt/TiO_2 facilitated by light pre-treatment, Catal. Sci. Technol. 6 (2016) 6679-6687.
[48] K. Wasa, M. Kitabatake, H. Adachi, Thin Film Materials Technology: Sputtering of Compound Materials, William Andrew, Inc., United States, 2004.
[49] H. Wender, P. Migowski, A.F. Feil, S.R. Teixeira, J. Dupont, Sputtering deposition of nanoparticles onto liquid substrates: Recent advances and future trends, Coord. Chem. Rev. 257 (2013) 2468-2483.
[50] S.V. Vladimirov, K. Ostrikov, A.A. Samarian, Fine Particles in Industrial Applications, Physics and Applications of Complex Plasmas, Imperial College Press, Singapore, 2005.

[51] P.H.V.D. Schaft, Chemical Conversions of Natural Precursors, in: R.G. Berger (Ed.), Flavours and Fragrances: Chemistry, Bioprocessing and Sustainability, Springer, Germany, 2007.
[52] Y. Pei, W. Huang, Bimetallic Nanostructures: Shape-Controlled Synthesis for Catalysis, Plasmonics, and Sensing Applications Wiley, India, 2018.
[53] L.J. Durndell, C.M.A. Parlett, N.S. Hondow, M.A. Isaacs, K. Wilson, A.F. Lee, Selectivity control in Pt-catalyzed cinnamaldehyde hydrogenation, Sci. Rep. 5 (2015) 9425.
[54] A. Sulman, P. Mäki-Arvela, L. Bomont, V. Fedorov, M. Alda-Onggar, A. Smeds, J. Hemming, V. Russo, J. Wärnå, M. Käldström, D.Y. Murzin, Vanillin Hydrodeoxygenation: Kinetic Modelling and Solvent Effect, Catalysis Letters 148 (2018) 2856-2868.

Figure captions

Figure 1. Selective hydrogenation of vanillin.

Figure 2. Schematic of the PDC-MSD system.

Figure 3. BET isotherms of the TiO_2 anatase support and all Pt/TiO_2 catalysts prepared by PDC-MSD.

Figure 4. H_2 temperature-programmed reduction profiles of the TiO_2 anatase support and all Pt/TiO_2 catalysts prepared by PDC-MSD and conventional impregnation.

Figure 5. XPS Pt 4f core level spectra of (a) Pt/TiO_2 MSD-45, (b) Pt/TiO_2 MSD-90, (c) Pt/TiO_2 MSD-135, (d) Pt/TiO_2 MSD-180, and (e) 0.4%Pt/TiO_2 IMP catalysts.

Figure 6. XPS Ti 2p core level spectra of (a) TiO_2 anatase support, (b) Pt/TiO_2 MSD-45, (c) Pt/TiO_2 MSD-90, (d) Pt/TiO_2 MSD-135, (e) Pt/TiO_2 MSD-180, (f) 0.1%Pt/TiO_2 IMP, and (g) 0.4%Pt/TiO_2 IMP catalysts.

Figure 7. XPS O 1s core level spectra of (a) TiO_2 anatase support, (b) Pt/TiO_2 MSD-45, (c) Pt/TiO_2 MSD-90, (d) Pt/TiO_2 MSD-135, (e) Pt/TiO_2 MSD-180, (f) 0.1%Pt/TiO_2 IMP, and (g) 0.4%Pt/TiO_2 IMP catalysts.

Figure 8. TEM micrographs of Pt/TiO_2 MSD-135 and Pt/TiO_2 MSD-180 catalysts.

Figure 9. Schematic proposed for the formation of Pt nanoparticles upon pulsed-DC magnetron sputtering deposition.

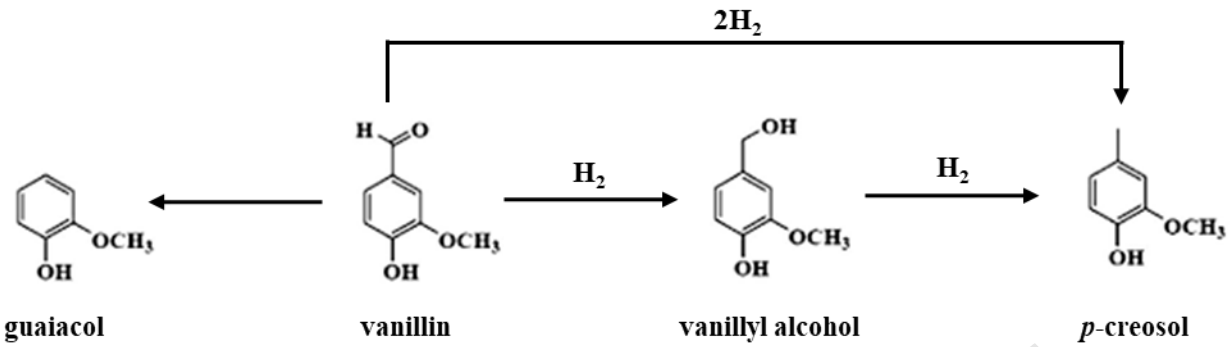

Figure 1.

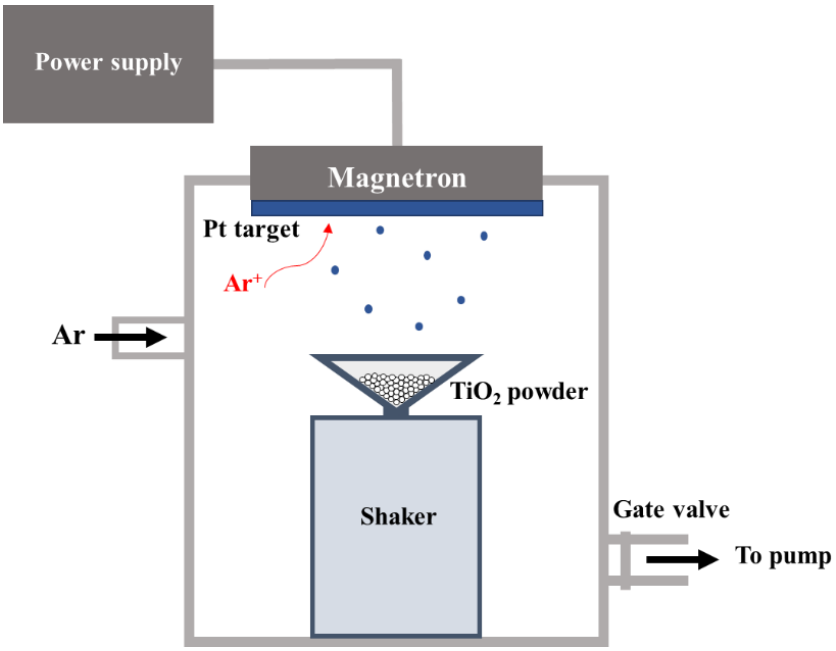

Figure 2.

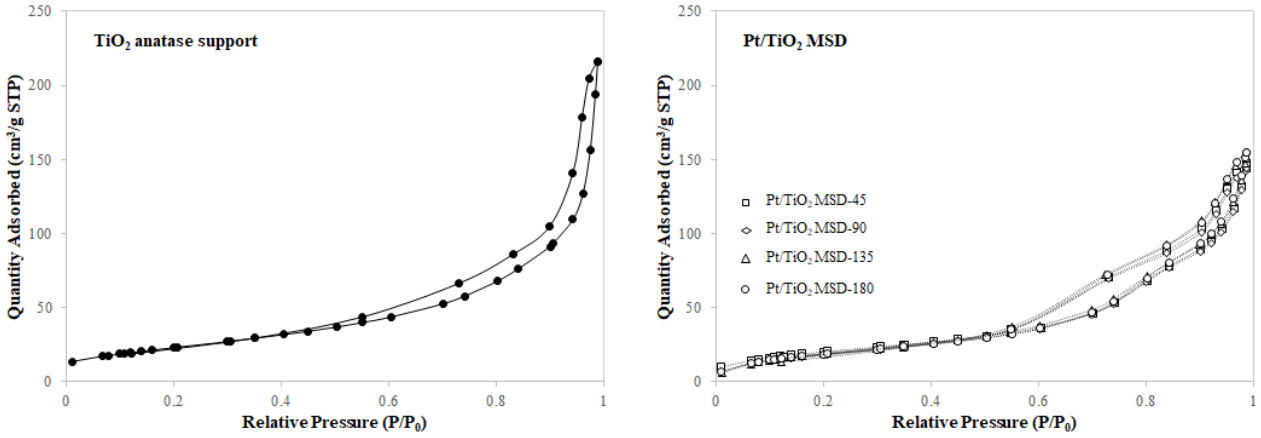

Figure 3.

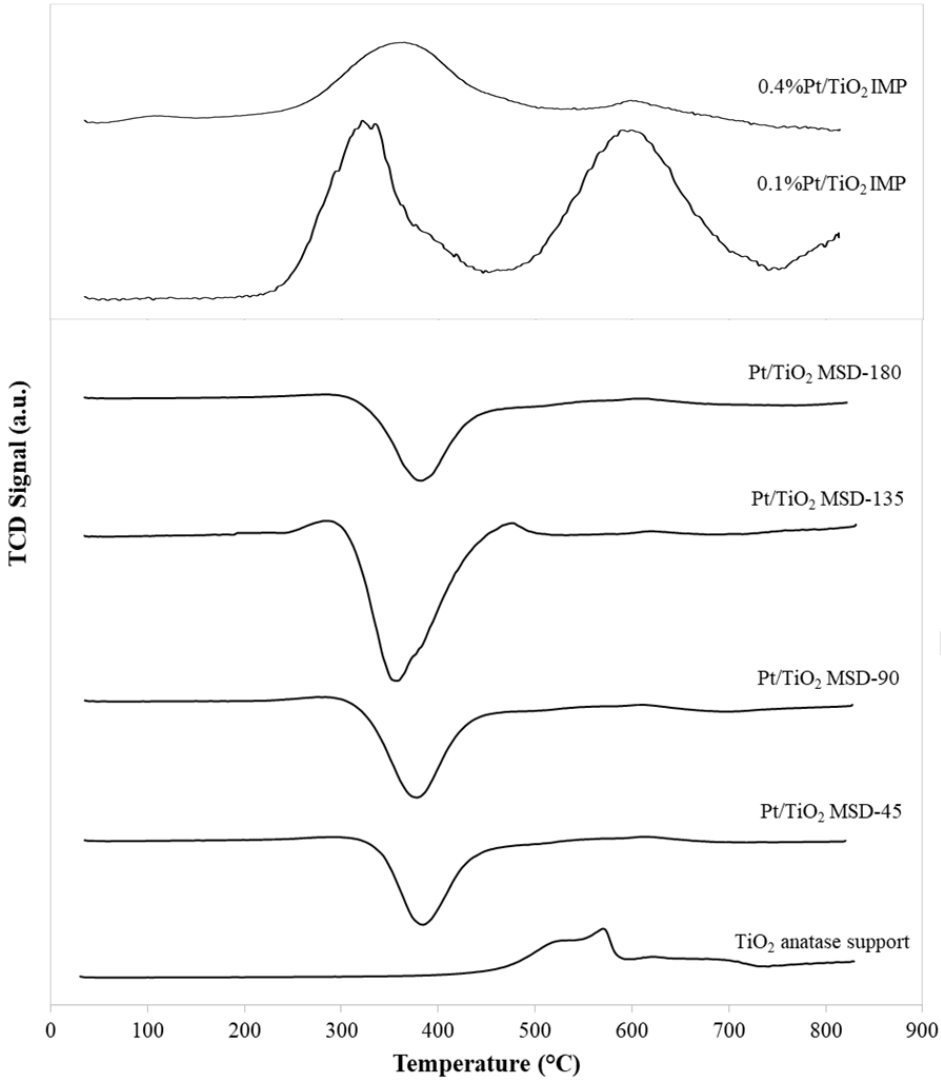

Figure 4.

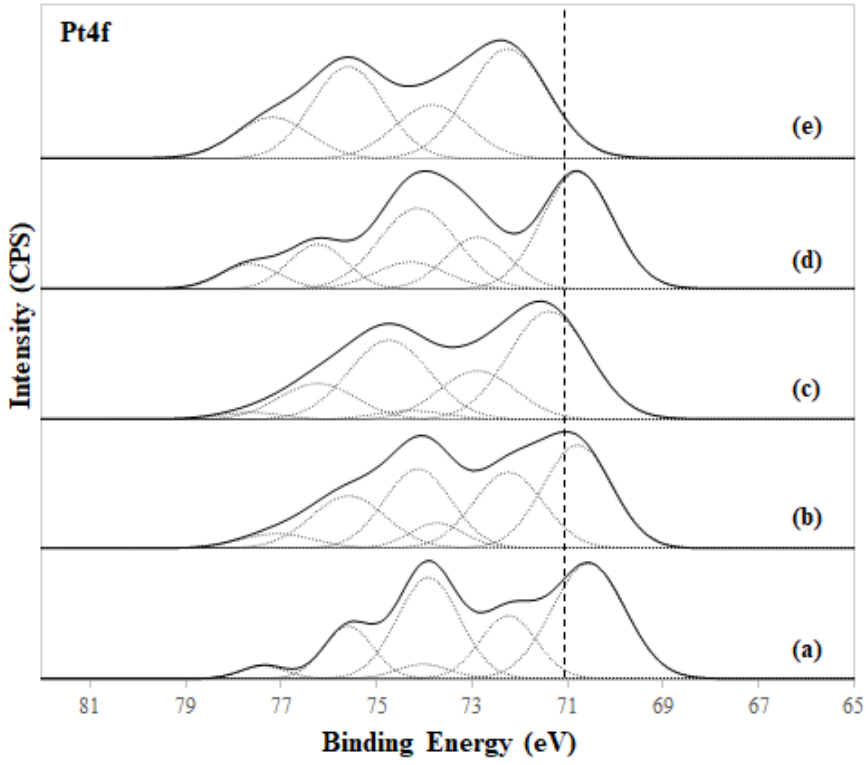

Figure 5.

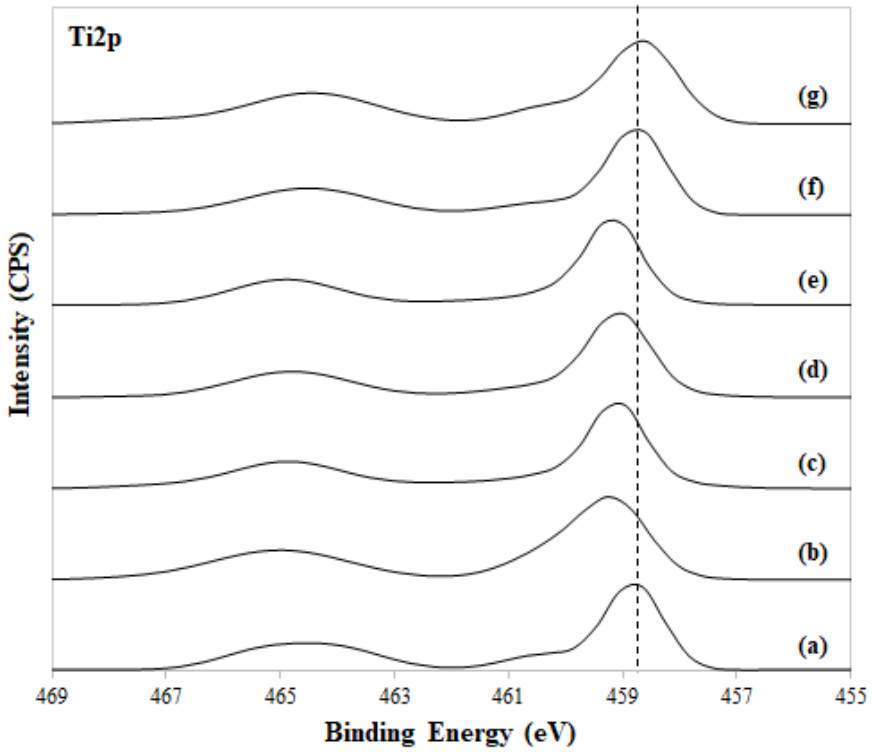

Figure 6.

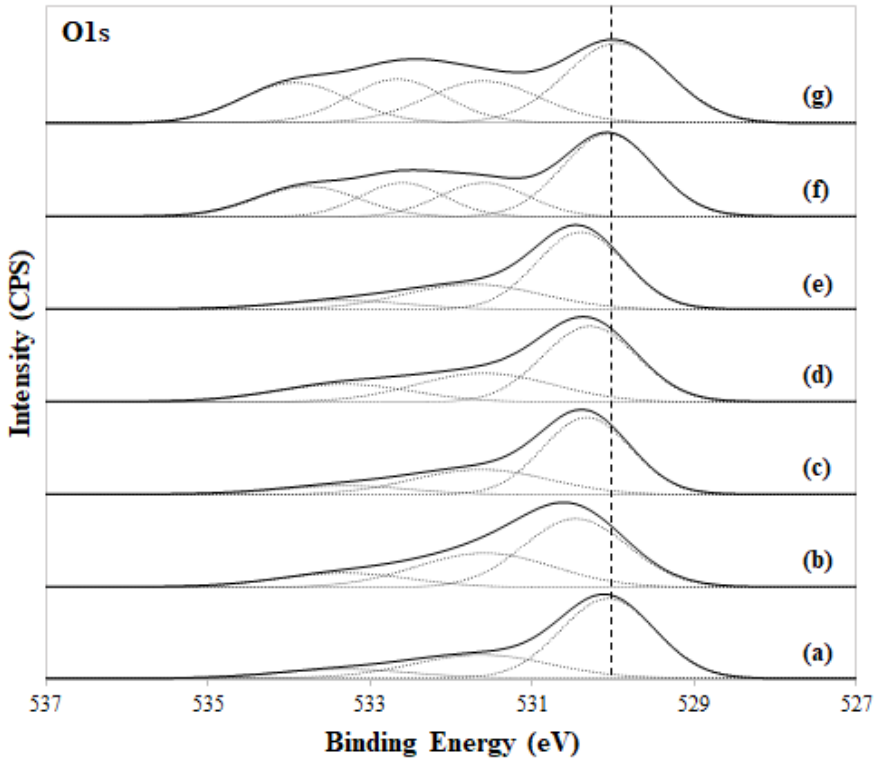

Figure 7.

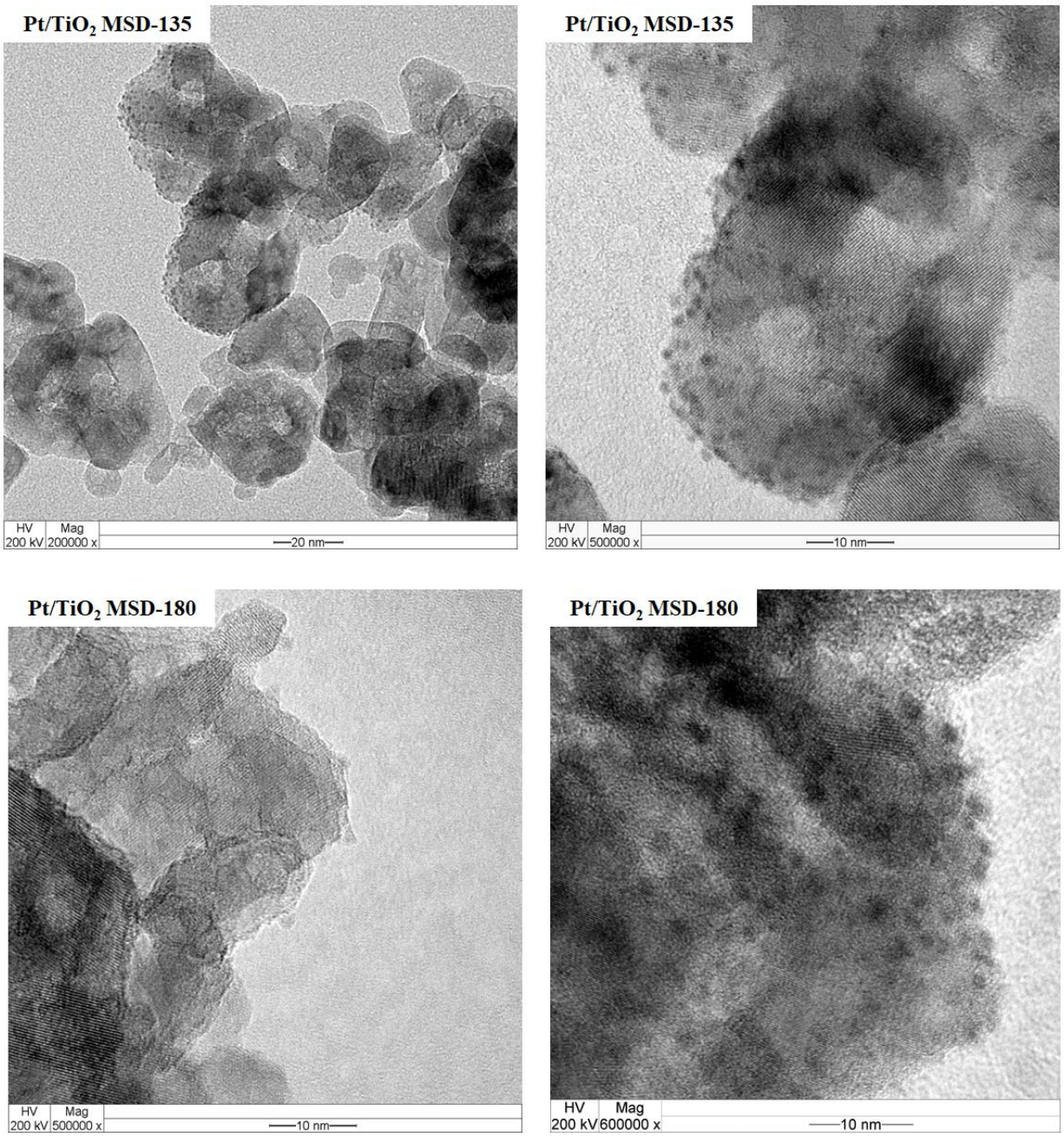

Figure 8.

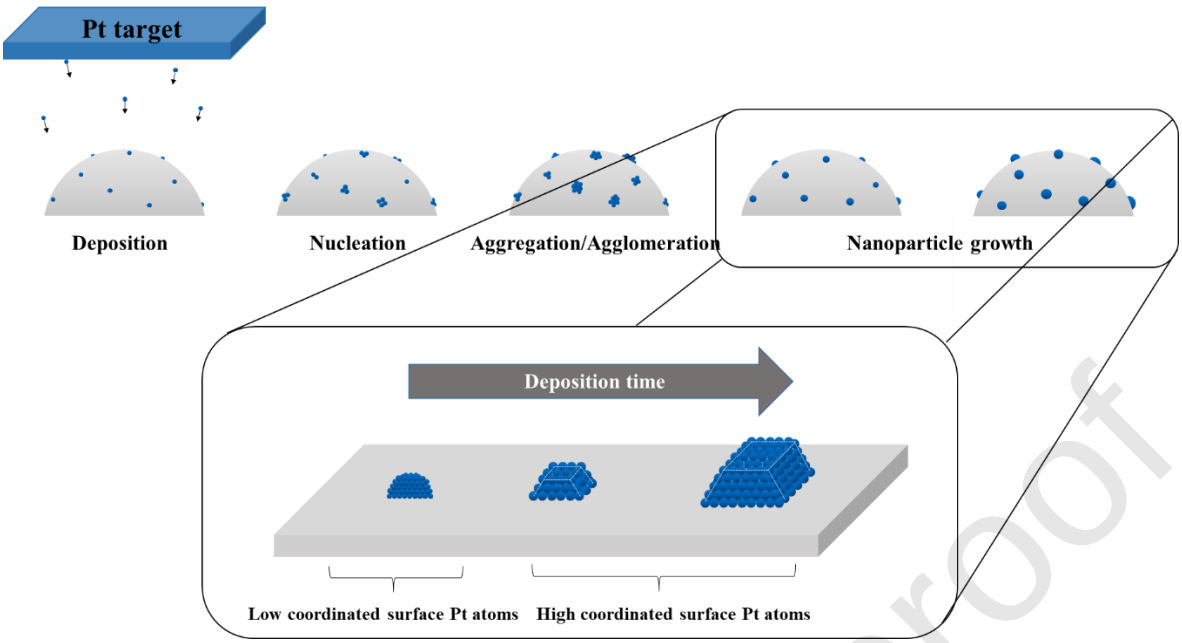

Figure 9.

Table 1. Actual Pt loadings under different deposition times and average metal deposition rate during PDC-MSD.

Catalyst	Deposition time (s)	Actual Pt loadings (wt.%)	Average deposition rate (μmol/s)
Pt/TiO_2 MSD-45	45	0.08	0.23
Pt/TiO_2 MSD-90	90	0.1	0.14
Pt/TiO_2 MSD-135	135	0.13	0.12
Pt/TiO_2 MSD-180	180	0.12	0.09

Table 2. N_2 physisorption properties of Pt deposited on TiO_2 by PDC-MSD with different deposition times.

Catalyst	Surface area (m^2/g)	Pore volume (cm^3/g)	Average pore diameter (nm)
TiO_2 anatase	85.3	0.33	11.5
Pt/TiO_2 MSD-45	75.9	0.23	8.2
Pt/TiO_2 MSD-90	71.3	0.22	8.0
Pt/TiO_2 MSD-135	74.6	0.23	7.6
Pt/TiO_2 MSD-180	72.1	0.24	8.2

Table 3. Atomic ratio of Pt/Ti and composition of different Pt species at catalyst surface for the Pt/TiO_2 prepared by PDC-MSD and conventional impregnation.

Catalyst	Atomic ratio Pt/Ti	Pt species		
		Pt metal (%)	PtO (%)	PtO_2 (%)
Pt/TiO_2 MSD-45	0.004	66.1	27.7	6.2
Pt/TiO_2 MSD-90	0.007	51.4	38.4	10.2
Pt/TiO_2 MSD-135	0.022	67.6	28.1	4.3
Pt/TiO_2 MSD-180	0.010	61.2	24.6	14.2
0.1%Pt/TiO_2 IMP	n.d.	n.d.	n.d.	n.d.
0.4%Pt/TiO_2 IMP	0.014	0	69.3	30.7

Table 4. Catalytic performances of the Pt/TiO_2 prepared by PDC-MSD and conventional impregnation in the liquid phase selective hydrogenation of vanillin under green conditions.

Catalyst	Reduction Temp. (ºC)	Conversion (%)	Selectivity (%)		
			Vanillyl alcohol	*p*-creosol	Guaiacol
Blank	-	0.9	100	-	-
Pt/TiO_2 MSD-45	-	15.1	100	-	-
Pt/TiO_2 MSD-90	-	19.1	98.1	1.9	-
Pt/TiO_2 MSD-135	-	58.1	97.9	2.1	-
	500	52.3	97.0	3.0	-
Pt/TiO_2 MSD-180	-	39.2	97.9	2.1	-
	500	34.4	97.9	2.1	-
0.1%Pt/TiO_2 IMP	500	46.1	98.4	1.6	-
0.4%Pt/TiO_2 IMP	500	81.8	97.9	2.1	-

Table 5. Comparison of the Pt/TiO_2 prepared by PDC-MSD, prepared by conventional impregnation, and reported in the literature for liquid phase selective hydrogenation of vanillin.

Catalysts	Metal loading (%wt.)	Preparation method	Reduction temperature (ºC)	Reaction conditions	Solvent	Reaction time (h)	Conversion (%)	Selectivity (%)	TON [b]	TOF (1/h) [c]	Ref.
Pt/TiO_2 MSD-135	0.13	PDC-MSD	-	70 ºC 2 MPa H_2	H_2O	2	58.1	97.9	4885	2442	This work
Pt/TiO_2 MSD-180	0.12	PDC-MSD	-	70 ºC 2 MPa H_2	H_2O	2	39.2	97.9	13939	6969	
0.1%Pt/TiO_2 IMP	0.1	IMP	500	70 ºC 2 MPa H_2	H_2O	2	46.1	98.4	2103	1051	
Pt/C [a]	5	Commerical (Degussa)	n/a	100 ºC 3 MPa H_2	H_2O	3	100	70	470	157	[12]
Pt/C [a]	5	Commercial (Degussa AG)	n/a	100 ºC 2.9 MPa H_2	H_2O	3	100	63	470	157	[54]

[a] Pt dispersion was 36.2%.
[b] TON was calculated based on mole of vanillin converted per mole of Pt active sites.
[c] TOF was calculated based on mole of vanillin converted per (mole of Pt active sites · time).